 CMC, vol.16, no.3, pp.229-246, 2010

Interface Effect on the Dynamic Stress around an Elliptical Nano-Inhomogeneity Subjected to Anti-Plane Shear Waves

Xue-Qian Fang[1,2], Xiao-Hua Wang[1] and Le-Le Zhang[3]

Abstract: In the design of advanced micro- and nanosized materials and devices containing inclusions, the effects of surfaces/interfaces on the stress concentration become prominent. In this paper, based on the surface/interface elasticity theory, a two-dimensional problem of an elliptical nano-inhomogeneity under anti-plane shear waves is considered. The conformal mapping method is then applied to solve the formulated boundary value problem. The analytical solutions of displacement fields are expressed by employing wave function expansion method, the expanded mode coefficients are determined by satisfying the boundary conditions at the interfaces of the nano-inhomogeneity. Analyses show that the effect of the interfacial properties on the dynamic stress is significantly related to the wave frequency of incident waves, the shear modulus ratio of the nano-inhomogeneity and the matrix, and the dimensions of the elliptical nano-inhomogeneity. Comparison with the previous results is also presented.

Keywords: Elliptical nano-inhomogeneity, Interface, Wave scattering, Dynamic stress concentration.

1 Introduction

Nanomaterials are categorized as those which have structured components with at least one dimension less than 100 nm. With the development of micro-fabrication and nanofabrication techniques, nanomaterials have found wide applications in electromechanical systems, bioengineering, optics and photonics, etc (Xie and Long, 2006) .

The classical theories of inclusions and inhomogeneities have been successfully applied to study the mechanical behavior of heterogeneous materials including piezo-

[1] Department of Engineering Mechanics, Shijiazhuang Railway Institute, Shijiazhuang, 050043, P.R. China

[2] Corresponding author. Tel.: +86 311 87936542; E-mail: fangxueqian@163.com

[3] School of Computing and Informatics, Shijiazhuang Railway Institute, Shijiazhuang, 050043, P.R. China

electricity problems (Chen et al., 2009). With the wide applications of nanocomposites in recent years, nanoscale inclusion/inhomogeneity theories have attracting more interests in recent years. Due to the increasing ratio of surface/interface area to the volume of nanocomposites, the surfaces and interfaces may have significant effects on the physical and mechanical properties of solids.

The effect of the mechanical behavior of surfaces and interfaces has been extensively studied in the past. Based on thermodynamics of solid surfaces, Gibbs (1906) took into consideration the effects of surface and interfacial energies. Subsequently, Gurtin and Murdoch (1975), Murdoch (1976) and Gurtin et al. (1998) developed a general theoretical framework for a continuum with surface stresses and proposed a linear surface stress-strain constitutive relation. The surface domain is assumed to be very thin and has different elastic moduli from the bulk, and the surface adheres to the bulk without slipping. In the following years, several other researchers have contributed to further development of the surface stress theory (e.g., Cahn and Larché, 1982; Cammarata, 1994; Nix and Gao, 1998, Sharma et al., 2003; Duan et al., 2005).

Recently, the stress concentration around the nano-inhomogeneity with surface/interface effect has attracted lots of interests. Wu et al. (2004) have studied the stress concentration near a nano-hole and the influence of a nano-hole on the elastic properties of a single crystal Ag from both atomistic and continuum viewpoints. A spherical nanocavity under a unidirectional remote tension (He and Li, 2006), a spherical nanoinclusion under a nonshear eigenstrain (Lim et al., 2006), and a cylindrical nanoinclusion under either a 2D dilatational eigenstrain or far-field loading (Tian and Rajapakse, 2007)were also studied. Cheng et al. (2009) investigated the effects of atomistic defects on the nanomechanical properties and fracture behaviors of single-walled CNTs (SWCNTs) using molecular dynamics (MD) simulation. For ellipsoidal inclusion, Liang et al. (2009) presented the solutions of the stress field around an ellipsoidal inclusion in the film/substrate half-space via the Fourier transforms and Stroh eigenrelation equations, and the effect of thin film's thickness on the stress field was analyzed. Using a tensor virial method of moments, an approximate solution to the relaxed elastic state of embedded ellipsoidal inclusions was given, and the surface/interface energies were considered (Sharma and Wheeler, 2007).

It can be found that most investigations focused on the nanocomposites under static loading. Due to the increasing demand of an understanding of dynamic processes in nanocomposites, it is highly desirable to study the stress in a fully dynamic framework. Recently, Wang et al. (2006) have investigated the diffraction of plane compressional waves by a nanosized circular hole with interface effects, and the dynamic stress around the hole was analyzed. Subsequently, this work was ex-

tended to the case of a spherical inclusion (Wang et al., 2007). However, no work treating the scattering of waves resulting from elliptical nano-inhomogeneities has been done. The solution for a nanoscale elliptical inhomogeneity in an infinite matrix is a very important fundamental problem in nanoscale solid mechanics as it is practically more useful than the solution for the idealized case of a circular or spherical inhomogeneity.

The objective of this paper is to investigate analytically the scattering of anti-plane shear waves from an elliptical nano-inhomogeneity with interface effects, and the dynamic stress around the nano-inhomogeneity is obtained. The wave fields around the nano-inhomogeneity are treated by complex function method. The displacement potentials are expressed by using wave function expansion method. The expanded mode coefficients are determined by satisfying the boundary conditions at the interface. The numerical solutions of the dynamic stress concentration factor are graphically illustrated. The effects of the incident wave frequency, the material properties of the inhomogeneities and the interface, and the shape of the elliptical nano-inhomogeneities on the dynamic stress around the nano-inhomogeneity are analyzed.

2 Problem formulation

Consider an infinite matrix material containing an elliptical nano-inhomogeneity with the semi-axis being a and b, respectively, as depicted in Fig.1. The origin of the Cartesian and polar coordinates is selected at the center of the elliptical nano-inhomogeneity. It is assumed that the matrix and the nano-inhomogeneity are both isotropic. The shear modulus and mass density of the nano-inhomogeneity are denoted by μ_0 and ρ_0, which are, in general, different from those (μ_m and ρ_m) of the matrix. In the surface/interface elasticity theory, a surface or interface is regarded as a negligibly thin layer adhered to the underlying matrix material. No slipping of the layer is permitted, and its elastic constants are different from those of the nano-inhomogeneity and matrix. The material properties of the surface/interface are denoted by μ_s and ρ_s. The matrix and inhomogeneity are denoted as the bulk. The elastic fields within the bulk solids satisfy the classical equilibrium equations, while the interface has its own elastic constants and is characterized by an additional constitutive law.

The dynamic excitation is provided by an anti-plane shear wave with frequency ω. The wave propagates along the x-direction. For the anti-plane problem in this study, only the displacement component in the $z$direction exists, i.e.,

$$u_x = u_y = 0, \quad u_z = w(x,y) \tag{1}$$

In the absence of body force, the anti-plane governing equation in the matrix is

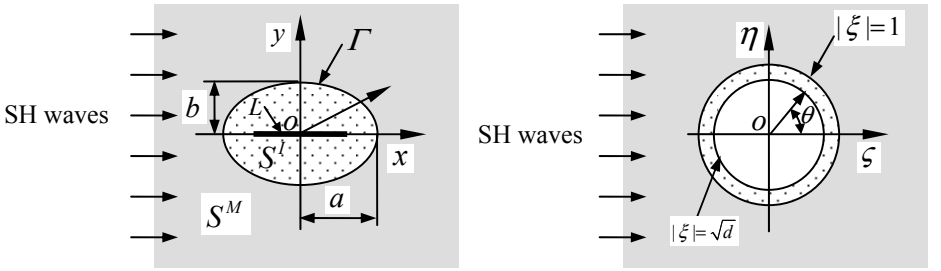

Figure 1: Geometry and coordinate systems of the problem

described as

$$\frac{\partial \tau_{zx}}{\partial x} + \frac{\partial \tau_{zy}}{\partial y} = \rho \frac{\partial^2 w}{\partial t^2} \tag{2}$$

where τ_{zx} and τ_{zy} are the shear stresses in the bulk.

The constitutive relations of anti-plane shear displacement are

$$\tau_{xz} = \mu \frac{\partial w}{\partial x}, \quad \tau_{yz} = \mu \frac{\partial w}{\partial y} \tag{3}$$

Substituting Eq.(3) into Eq.(2), the following equation can be obtained

$$\frac{\partial^2 w}{\partial x^2} + \frac{\partial^2 w}{\partial y^2} = \frac{\rho}{\mu} \frac{\partial^2 w}{\partial t^2} \tag{4}$$

The steady solution of this problem is considered. It is supposed that $w = We^{-\mathrm{i}\omega t}$, then Eq.(4) is expressed as

$$\nabla^2 W + k^2 W = 0 \tag{5}$$

where $\nabla^2 = \partial^2/\partial x^2 + \partial^2/\partial y^2$ is the two-dimensional Laplacian operator, and $k = \omega/c$ with $c = \sqrt{\mu_m/\rho_m}$is the wave number of shear waves in the matrix.

To apply complex function method, the complex variable $z = x + \mathrm{i}y$ and its complex conjugate $\bar{z} = x - \mathrm{i}y$ are introduced. Then the following relations can be obtained

$$\frac{\partial}{\partial x} = \frac{\partial}{\partial z} + \frac{\partial}{\partial \bar{z}}, \quad \frac{\partial}{\partial y} = \mathrm{i}\left(\frac{\partial}{\partial z} - \frac{\partial}{\partial \bar{z}}\right) \tag{6}$$

The wave equation (5) can be expressed with respect to the variables z and $\bar{z}$, i.e.,

$$4\frac{\partial^2 W}{\partial z \partial \bar{z}} + k^2 W = 0 \tag{7}$$

Then the displacement W, shear stresses τ_{xz}, τ_{yz}, τ_{nz},τ_{tz} in the matrix and nano-inhomogeneity can be expressed in terms of the analytical function $f(z)$ as

$$W = \frac{f(z) + \overline{f(z)}}{2} \tag{8}$$

$$\tau_{xz} - i\tau_{yz} = \mu f'(z) \tag{9}$$

$$\tau_{nz} - i\tau_{tz} = \mu e^{i\theta} f'(z) \tag{10}$$

where $f'(z)$ denotes the derivative with respect to the argument z.

3 Micromechanical framework for surface/interface stress

An elastically isotropic interface is considered. According to the theory of Gurtin and Murdoch (1975) and Gurtin et al. (1998), the elastic field within the interface has its own elastic constants and is described by an additional constitutive law.

As the current problem is of anti-plane nature, the equilibrium equations and the surface/interface stresses for an isotropic surface/interface are given by

$$\tau_{nz}^{(M)} - \tau_{nz}^{(I)} + \frac{\partial \tau_{tz}^{S}}{\partial t} = 0 \tag{11}$$

$$\tau_{tz}^{S} = 2(\mu_s - \tau_0)\varepsilon_{tz}^{S} \tag{12}$$

where μ_s is the shear modulus of the interface, t is the unit tangent of the boundary Γ, n is the outward unit normal at the interface. τ_{tz}^{S} is the interfacial stress components, ε_{tz}^{S} is the interfacial strain component, and τ_0 is the residual surface stress under unstrained conditions. It should be noted that for all the quantities below, the superscripts I, M, and S denote the nano-inhomogeneity, the matrix and the interface, respectively.

In this paper, a coherent interface is considered. For a coherent interface, the interface strain is equal to the tangential strain in the abutting bulk materials, i.e.,

$$\varepsilon_{tz}^{S}(z_\Gamma) = \varepsilon_{tz}^{M}(z_\Gamma) = \varepsilon_{tz}^{I}(z_\Gamma), \quad z_\Gamma \in \Gamma \tag{13}$$

where $z_\Gamma = x_\Gamma + iy_\Gamma$ denotes the points at the interface.

Thus, Eq.(11) can be rewritten as

$$\tau_{nz}^{(I)} - \tau_{nz}^{(M)} = \frac{\mu_s - \tau_0}{\mu_M} \frac{\partial \tau_{tz}^{M}}{\partial t} \tag{14}$$

Eq. (14) forms a non-classical boundary condition at the inhomogeneity-matrix interface. Since the residual surface stress τ_0 always induces an additional deformation filed, and is independent of the external loading, it is assumed the residual surface stress is zero.

4 Conformal mapping method

In this section, the mapping function of transforming the elliptical boundary between the nano-inhomogeneity and the matrix into a unit circle is introduced, shown in Fig.1. The expression of z is written as

$$z = g(\xi) = c(\xi + d/\xi), \quad \xi = \varsigma + \mathrm{i}\eta = re^{\mathrm{i}\theta} \tag{15}$$

Here $e^{\mathrm{i}\theta} = \frac{g(\xi)}{|g(\xi)|}$, $c = (a+b)/2$, $d = (a-b)/(a+b)$ and $0 \le d \le 1$. The mapping function transforms the region S^Minto the exterior region of a unit circle $|\xi| = 1$, and region S^1into an annular region between the unit circle and a circle of radius $|\xi| = \sqrt{d}$. Here the region S^1 is imagined to be cut along the line $L = \{(x,0)| -l \le x \le l\}$, which is transformed into a circle of radius $\sqrt{d}$.

From Eq.(10), the shear stress in the $(z,\bar{z})$ plane can be rewritten as

$$\tau_{nz} = \frac{\mu}{2}\left(\xi\frac{\partial W}{\partial z} + \bar{\xi}\frac{\partial W}{\partial \bar{z}}\right), \quad \tau_{tz} = \frac{\mathrm{i}\mu}{2}\left(\xi\frac{\partial W}{\partial z} - \bar{\xi}\frac{\partial W}{\partial \bar{z}}\right) \tag{16}$$

The derivatives with respect to the tangential direction t can be expressed as

$$\frac{\partial}{\partial t} = \frac{\partial}{\partial z}\frac{\partial z}{\partial t} + \frac{\partial}{\partial \bar{z}}\frac{\partial \bar{z}}{\partial t}, \quad \frac{\partial z}{\partial t} = \mathrm{i}e^{\mathrm{i}\theta}, \quad \frac{\partial \bar{z}}{\partial t} = -\mathrm{i}e^{-\mathrm{i}\theta} \tag{17}$$

5 The wave fields around the elliptical inhomogeneity in the nano-sized material

Following the standard wave function expansion method, the wave fields in the nano-sized material can be expressed.

5.1 Incident waves

Consider an anti-plane shear wave propagating along the positive$x$direction. It is convenient for us to express the displacement in the cylindrical coordinate system, i.e.,

$$W^{(in)} = W_0 e^{\mathrm{i}kx} = W_0 \sum_{n=-\infty}^{\infty} \mathrm{i}^n J_n(k|g(\xi)|)\left[\frac{g(\xi)}{|g(\xi)|}\right]^n \tag{18}$$

where W_0 is the amplitude of incident waves, and $J_n(\bullet)$ is the nth Bessel function of the first kind. It is noted that all field quantities have the same time variation $e^{-\mathrm{i}\omega t}$ which is suppressed in all subsequent representations for notational convenience.

5.2 The scattered field of anti-plane shear waves

When the incident waves propagate in the small-sized material with nano-inhomogeneities, the scattered waves around the nano-inhomogeneities come into being. The displacement field of the scattered waves is given by

$$W^{(s)} = W_0 \sum_{n=-\infty}^{\infty} A_n H_n^{(1)}(k|g(\xi)|) \left[\frac{g(\xi)}{|g(\xi)|}\right]^n \tag{19}$$

where A_n are the mode coefficients of scattered waves around the nan-ohomogeneity, $H_n^{(1)}(\bullet)$ is the nth Hankel function of the first kind, and denotes the outgoing propagating waves.

5.3 The refracted field inside the nano-inhomogeneity

The refracted waves, being confined inside the elliptical nano-inhomogeneity, are standing waves, and represented by

$$W^{(r)} = W_0 \sum_{n=-\infty}^{\infty} B_n J_n(k_0|g(\xi)|) \left[\frac{g(\xi)}{|g(\xi)|}\right]^n \tag{20}$$

where $k_0 = \omega/c_0$ with $c_0 = \sqrt{\mu_0/\rho_0}$ is the wave number in the inhomogeneity, and the cylindrical Bessel functions of the first kind are used to obtain the standing waves.

The total wave field in the matrix material is produced by the superposition of the incident and the scattered waves resulting from the nano-inhomogeneties,

$$W^{(t)} = W^{(in)} + W^{(s)} \tag{21}$$

Then, in the complex plane $(z, \bar{z})$, the shear stresses in the normal direction resulting from the incident, the scattered, and the refracted waves are expressed as

$$\begin{aligned}\tau_{nz}^{(in)} &= \frac{\mu_m k W_0}{2} \\ &\sum_{n=-\infty}^{\infty} \mathrm{i}^n \left[J_{n-1}(k_0|g(\xi)|)\left(\frac{g(\xi)}{|g(\xi)|}\right)^{n-1} - J_{n+1}(k|g(\xi)|)\left(\frac{g(\xi)}{|g(\xi)|}\right)^{-(n+1)}\right]\frac{\xi g'(\xi)}{|g'(\xi)|} \\ &\left[J_{n-1}(k_0|g(\xi)|)\left(\frac{g(\xi)}{|g(\xi)|}\right)^{n-1} - J_{n+1}(k|g(\xi)|)\left(\frac{g(\xi)}{|g(\xi)|}\right)^{n+1}\right]\frac{\bar{\xi}\overline{g'(\xi)}}{|g'(\xi)|}\end{aligned} \tag{22}$$

$$\tau_{nz}^{(s)} = \frac{\mu_m k W_0}{2} \sum_{n=-\infty}^{\infty} A_n \left[H_{n-1}^{(1)}(k|g(\xi)|) \left(\frac{g(\xi)}{|g(\xi)|} \right)^{n-1} \frac{\xi g'(\xi)}{|g'(\xi)|} - H_{n+1}^{(1)}(k|g(\xi)|) \left(\frac{g(\xi)}{|g(\xi)|} \right)^{n+1} \frac{\bar{\xi}\overline{g'(\xi)}}{|g'(\xi)|} \right] \tag{23}$$

$$\tau_{nz}^{(r)} = \frac{\mu_0 k_0 W_0}{2} \sum_{n=-\infty}^{\infty} B_n \left[J_{n-1}(k_0|g(\xi)|) \left(\frac{g(\xi)}{|g(\xi)|} \right)^{n-1} \frac{\xi g'(\xi)}{|g'(\xi)|} - J_{n+1}(k|g(\xi)|) \left(\frac{g(\xi)}{|g(\xi)|} \right)^{n+1} \frac{\bar{\xi}\overline{g'(\xi)}}{|g'(\xi)|} \right] \tag{24}$$

$$\tau_{tz}^{(in)} = \frac{\mu_m k W_0}{2} \sum_{n=-\infty}^{\infty} \mathrm{i}^{n+1} \left[J_{n-1}(k|g(\xi)|) \left(\frac{g(\xi)}{|g(\xi)|} \right)^{n-1} \frac{\xi g'(\xi)}{|g'(\xi)|} + J_{n+1}(k|g(\xi)|) \left(\frac{g(\xi)}{|g(\xi)|} \right)^{n+1} \frac{\bar{\xi}\overline{g'(\xi)}}{|g'(\xi)|} \right] \tag{25}$$

$$\tau_{tz}^{(s)} = \frac{\mathrm{i}\mu_m k W_0}{2} \sum_{n=-\infty}^{\infty} A_n \left[H_{n-1}^{(1)}(k|g(\xi)|) \left(\frac{g(\xi)}{|g(\xi)|} \right)^{n-1} \frac{\xi g'(\xi)}{|g'(\xi)|} + H_{n+1}^{(1)}(k|g(\xi)|) \left(\frac{g(\xi)}{|g(\xi)|} \right)^{n+1} \frac{\bar{\xi}\overline{g'(\xi)}}{|g'(\xi)|} \right] \tag{26}$$

6 The boundary conditions of the elliptical nano-inhomogeneity

On the interface ($\xi = e^{\mathrm{i}\theta}$), the displacements around the elliptical nano-inhomogeneity should be continuous, i.e.,

$$W^{(t)}|_{z=g(\xi)} = W^{(r)}|_{z=g(\xi)} \tag{27}$$

The equilibrium equations with interface effects around the elliptical nano-inhomogeneity is rewritten as

$$\left[\xi \frac{\partial W^{(t)}}{\partial z} + \bar{\xi} \frac{\partial W^{(t)}}{\partial \bar{z}} \right] - f_0 \left[\xi \frac{\partial W^{(r)}}{\partial z} + \bar{\xi} \frac{\partial W^{(r)}}{\partial \bar{z}} \right] = f_s \left[\xi \frac{\partial \Delta}{\partial z} - \bar{\xi} \frac{\partial \Delta}{\partial \bar{z}} \right] \tag{28}$$

where $f_0 = \mu_0/\mu_m, f_s = \mu_s/\mu_m$, and $\Delta = \xi \frac{\partial W^{(t)}}{\partial z} - \bar{\xi} \frac{\partial W^{(t)}}{\partial \bar{z}}$.

Substituting Eqs.(18)-(20) into Eqs.(27)-(28), the mode coefficients A_n and B_n can be determined. In the surface elasticity theory, the parameter f_s is an important index standing for the surface effects. The surface elastic modulus can be determined by molecular dynamics simulations or experiments. Atomic simulations of fcc Al, diamond Si, and some other materials showed that surface elastic modulus can be either positive or negative, depending on the crystallographic structure, and that the absolute values of f_s is on the order of angstroms (Miller and Shenoy, 2000; Sharma et al., 2003). Therefore, for a macroscopic inclusion with a big values of $a$and$b$ and $k \ll 1$, the surface effects can be neglected and then Eqs.(27) and (28) reduce to the boundary conditions in classical elasticity. However, when the radius of hole shrinks to nanometers, f_s becomes noticeable and the surface effects should be taken into consideration.

7 Determination of mode coefficients and dynamic stress concentration factor

By satisfying the boundary conditions (27)-(28) at the interface of the nano-inhomogeneity, the mode coefficients of scattered and refracted waves are determined. Substituting Eqs.(18)-(24) into Eqs.(27)-(28), and making use of the orthogonal relation of $e^{-\mathrm{i}s\theta}$, a set of algebraic equations is obtained. After arrangement, the equations can be simplified as

$$[E_s]\{X_s\} = \{f_s\}, \quad s = 0, \pm 1, \pm 2, ..., \propto \tag{29}$$

where $[E_s]$ is a matrix, $\{X_s\} = \{A_s, B_s\}^T$. Using Eq.(28), the scattering and refracting coefficients are determined.

In the presence of nano-inhomogeneity, the stress field shows significantly difference due to the refraction and scattering of waves. According to the definition of the dynamic stress concentration factor (*DSCF*), the *DSCF* is the ratio of the tangent stress around the nano-inhomogeneity to the maximum stress of the incident waves (Pao and Mow, 1973). Thus, the dimensionless *DSCF* around the cylindrical nano-inhomogeneity is expressed as

$$DSCF = \frac{\tau_{tz}}{\tau_0} \tag{30}$$

where $\tau_{tz} = \tau_{tz}^{(in)} + \tau_{tz}^{(s)}$, $\tau_0 = \mu_m k W_0$ denotes the maximum stress resulting from the incident waves. The results have the general form of $DSCF = (R + \mathrm{i}I)e^{-\mathrm{i}\omega t}$, whose absolute value $(R + \mathrm{i}I)^{1/2}$ is the maximum dynamic stress concentration factor.

8 Numerical examples and analysis

Fatigue failures often occur in the regions with high stress concentration, so an understanding of the distribution of the dynamic stress around the nano-inhomogeneity is very useful in structural design. Due to the symmetry about the x-axis of the elliptical nano-inhomogeneity and the incident direction of shear waves, only the dynamic stress distribution at the positions of $y \geq 0$ is illustrated in the following numerical analysis.

In the numerical analysis, it is convenient to make the variables dimensionless. To this end, we may introduce a characteristic length a, where a is the semi-axis length of the elliptical nano-inhomogeneity. The following dimensionless variables and quantities have been chosen for computation: the incident wave number is $k^* = ka = 0.01 - 2.0$, the shear modulus ratio of the nano-inhomogeneity and the matrix is $f_0 = \mu_0/\mu_m = 0.1 - 10$, the shear modulus ratio of the nano-inhomogeneity and the matrix is $f_s = \mu_s/\mu_m = 0.1 - 10$, the density ratio is $\rho = \rho_0/\rho_m = 1.0 - 3.0$ and the values of $b$is $b^* = b/a = 0.1 - 6.0$.

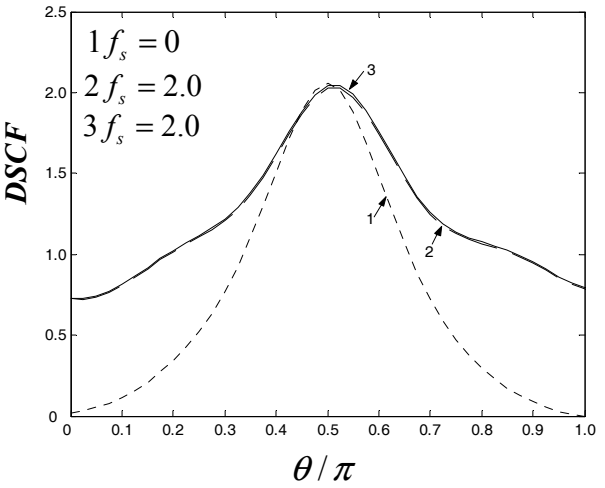

Figure 2: Dynamic stress concentration factor around the elliptic nano-inhomogeneity $(k^* = 0.05, b^* = 1.0, f_0 = 3.0, \rho = 2.0)$ 1 and 2-obtained from this paper; 3- obtained from Tian and Rajapakse (2007)

In order to validate the present dynamical model, comparison with the previous literatures is given. Fig.2 shows the angular distribution of the dynamic stress around the nano-inhomogeneity with parameters: $k^* = 0.05$, $b^* = 1.0$, $f_0 = 3.0$, $\rho = 2.0$,

and $b^* = 1.0$. When $k^* = 0.05$, the dynamic excitation is reduced to the steady case. If the values of $a$and b are the same, i.e., $b^* = 1.0$, the elliptical nano-inhomogeneity becomes a circular nano-inhomogeneity. $f_s = 0$ means that the interface effect is ignored. It can be seen that the angular distribution of *DSCF*s is symmetric about the two axes. In the case of $f_s = 0$, the maximum dynamic stress occurs at the position of $\theta = \pi/2$, and the maximum value of dimensionless dynamic stress is about 1.95. These conclusions are consistent with those in Pao and Mow (1973). In Pao and Mow (1973), no interface effect is considered. Through comparison, it is also found that when the interface effect is considered, the dynamic stresses at the positions near $\theta = 0, \pi$ increase greatly. The variation of dynamic stresses at other positions is little. Comparing with the results in Tian and Rajapakse (2007), the good agreements can be found in Fig.2.

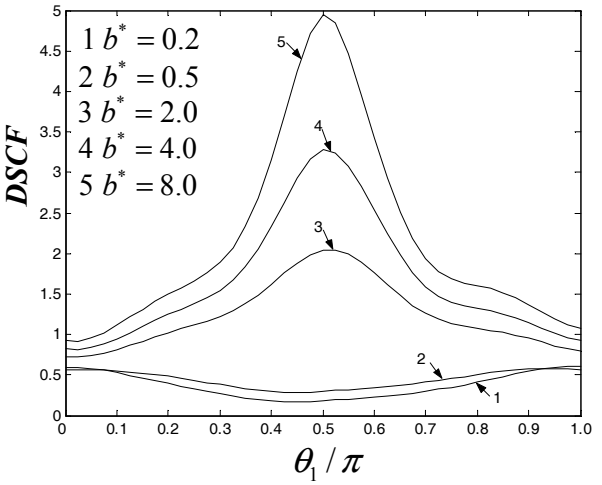

Figure 3: Dynamic stress concentration factor around the elliptic nano-inhomogeneity with different values of b^* $(k^* = 0.1, f_0 = 3.0, f_s = 2.0, \rho = 2.0)$

Fig.3 illustrates the distribution of *DSCF* around the elliptical nano-inhomogeneity when the value of b^* is different in the region of low frequency. It can be seen that when the value of b^* is greater than 1.0, namely b is the long semi-axis, the maximum dynamic stress increases greatly with the increase of b^*. At the positions near $\theta = \pi/2, 3\pi/2$, the variation of dynamic stress in the greatest. When the value of b^* is less than 1.0, namely a is the long semi-axis, the maximum dynamic stress occurs at the positions near $\theta = 0, \pi$. However, comparing with the case of $b^* > 1.0$, the variation of dynamic stress around the elliptical nano-inhomogeneity

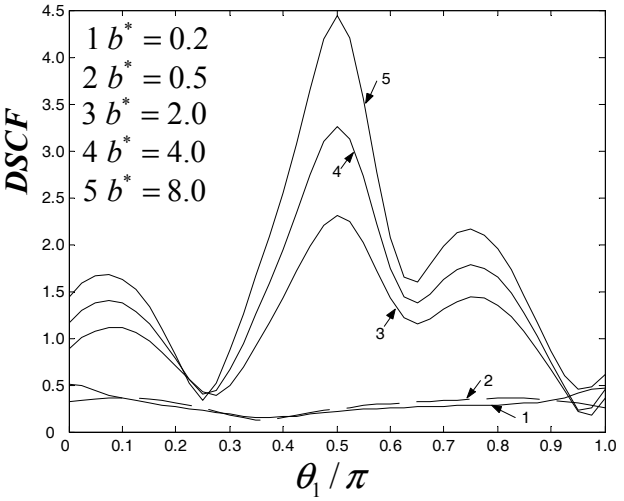

Figure 4: Dynamic stress concentration factor around the elliptic nano-inhomogeneity with different values of b^* ($k^* = 1.5, f_0 = 3.0, f_s = 2.0, \rho = 2.0$)

is less.

Fig.4 illustrates the distribution of *DSCF* around the elliptical nano-inhomogeneity when the value of b^* is different in the region of high frequency. It can be seen that when the value of b^* is greater than 1.0, namely b is the long semi-axis, the maximum dynamic stress increases greatly with the increase of b^*. However, more peaks of dynamic stress occur when the frequency of waves is high. Comparing with the results in Fig.3, it is found that the shape of the elliptical nano-inhomogeneity decreases in the region of high frequency. When the value of b^* is less than 1.0, the dynamic stress around the elliptical nano-inhomogeneity shows little variation with the value of b^*.

Fig.5 illustrates the distribution of *DSCF* around the elliptical nano-inhomogeneity with different wave frequencies of incident waves. It can be seen that in the region of low frequency, the variation of the dynamic stress around the elliptical nano-inhomogeneity is great, especially at the positions near $\theta = \pi/2, 3\pi/2$. The maximum dynamic stress increases with the increase of wave frequency. However, in the region of high frequency, more peaks occur around the elliptical nano-inhomogeneity. The dynamic stress around the nano-inhomogeneity decreases. The variation of dynamic stress around the nano-inhomogeneity is also less than that in low frequencies. This phenomenon is due to the scattering and refraction of shear waves around the nano-inhomogeneity. With the increase of wave frequency,

the scattering and refraction of shear waves around the nano-inhomogeneity become stronger. The interference between the incident and scattering waves becomes more important.

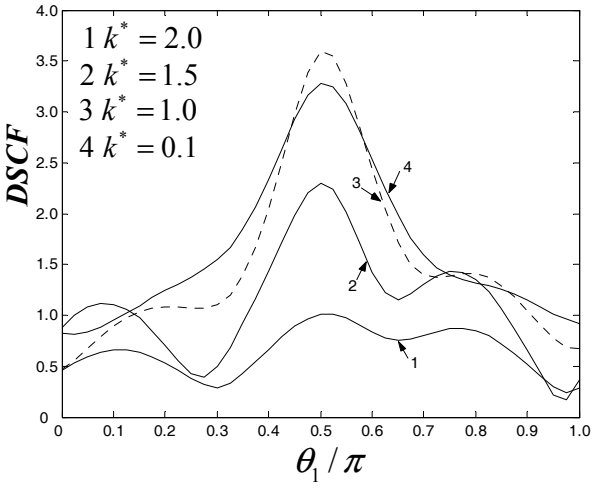

Figure 5: Dynamic stress concentration factor around the elliptic nano-inhomogeneity with different values of k^* ($b^* = 2.0, f_0 = 3.0, f_s = 2.0, \rho = 2.0$)

Figs.6 and 7 illustrate the distribution of *DSCF* around the elliptical nano-inhomogeneity with different values of f_0. It can be seen that in the region of low frequency, the dynamic stress around the elliptical nano-inhomogeneity increases when the nano-inhomogeneity is stiffer than the matrix. In the region of high frequency, the value of f_0 expresses greater effect on the dynamic stress at the positions near $\theta = \pi$. This phenomenon results from the strong scattering and refraction of waves.

To find the interface effect on the dynamic stress around the elliptical nano-inhomogeneity with different wave frequencies of incident waves, Figs.8 and 9are given. Fig.8 shows the dynamic stress around the elliptical nano-inhomogeneity in the region of low frequency. It can be seen that the dynamic stress increases with the increase of the value of f_s. At the positions near $\theta = \pi/2, 3\pi/2$, the effect of interface on the dynamic stress is greater. Fig.9 shows the dynamic stress around the elliptical nano-inhomogeneity in the region of high frequency. Comparing with the results in Fig.8 it is clear that the interface effect on the dynamic stress decreases in the region of high frequency. At the positions near $\theta = 0$, the variation of dynamic stress is little. This phenomenon results from the strong scattering and refraction of waves at this position. However, at the positions near $\theta = 0$, with the decrease of

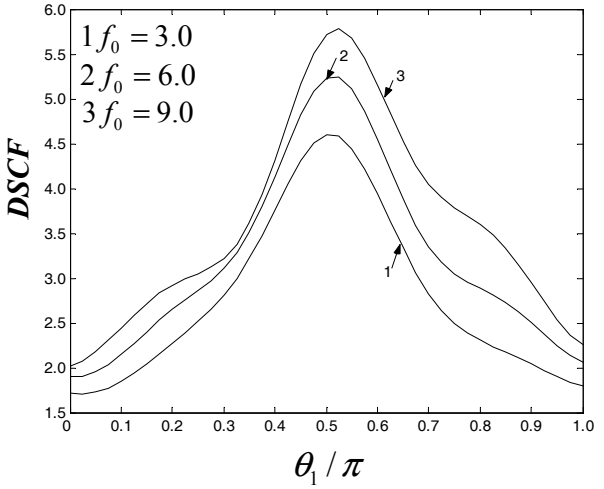

Figure 6: Dynamic stress concentration factor around the elliptic nano-inhomogeneity with different values of f_0 $(k^* = 0.1, b^* = 2.0, f_s = 2.0, \rho = 2.0)$

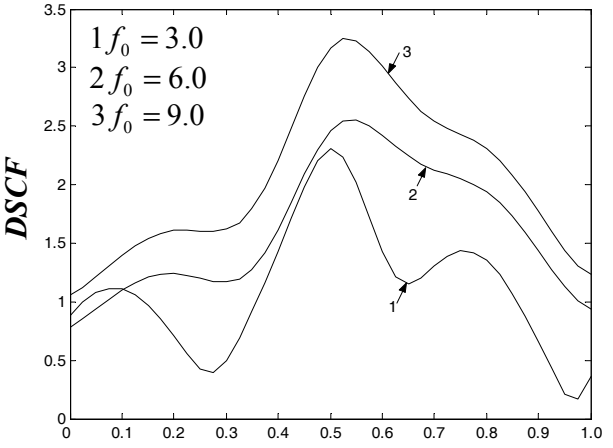

Figure 7: Dynamic stress concentration factor around the elliptic nano-inhomogeneity with different values of f_0 $(k^* = 1.5, b^* = 2.0, f_s = 2.0, \rho = 2.0)$

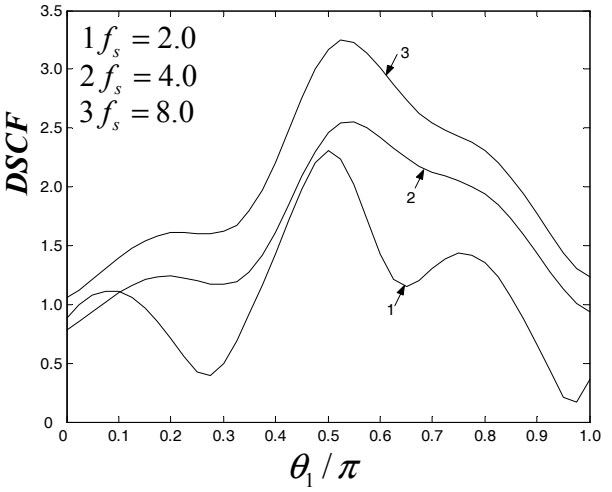

Figure 8: Dynamic stress concentration factor around the elliptic nano-inhomogeneity with different values of f_s $(k^* = 0.2, b^* = 2.0, f_0 = 3.0, \rho = 2.0)$

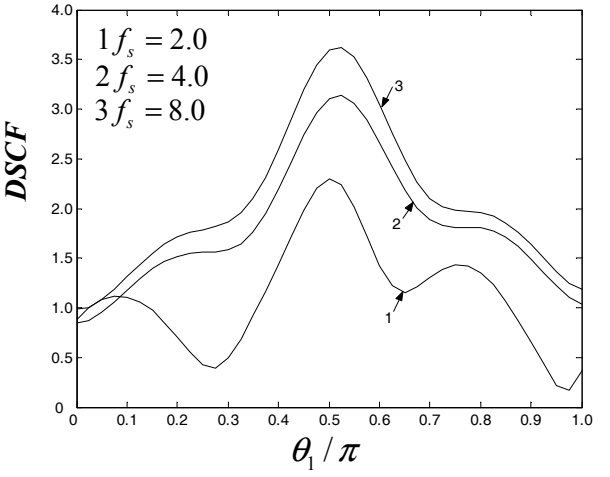

Figure 9: Dynamic stress concentration factor around the elliptic nano-inhomogeneity with different values of f_s $(k^* = 1.5, b^* = 2.0, f_0 = 3.0, \rho = 2.0)$

scattering and refraction effects of waves, the interface effect on the dynamic stress is great.

9 Conclusion

In this study, the interface model of Gurtin and Murdoch Gurtin's has been adopted to investigate the diffraction of anti-plane shear wave by an elliptical nanosized inhomogeneities, and the effect of interfacial properties on the dynamic stress around the nano-inhomogeneities under different region of frequencies is analyzed. Comparison with the previous investigations validates this present model. Through analyzing the interface effect on the dynamic stress of nanosized material under shear waves, the methods of reducing the dynamic stress and increasing the strength of nanosized structures are found.

It has been found that the surface/interface elasticity shows significant effects on the dynamic stress around the nano-inhomogeneity. In the region of lower frequencies, the effects are greater. The effect of the shear modulus ratio on the dynamic stress is also related to the surface/interface elasticity when the inclusion size shrinks to nanometers. If the nano-inhomogeneties are stiffer than the matrix, the effect is greater. When b is the long semi-axis, the maximum dynamic stress increases greatly with the increase of b^*. When a is the long semi-axis, variation of dynamic stress around the elliptical nano-inhomogeneity is less. In the region of high frequency, the interference between the incident and scattering waves becomes distinct. The effects of the interface properties and the shape of the elliptical nano-inhomogeneity on the dynamic stress decrease with the increase of wave frequency. The variation of the dynamic stress around the elliptical nano-inhomogeneity also decreases when the wave frequency is higher.

Acknowledgement: The paper is supported by the Natural Science Foundation of Hebei Province, China (Foundation No. A2010001052), and the Program for Changjiang Scholars and Innovative Research Team in University.

10 References

Cahn, J.W.; Larché, F. (1982): Surface stress and chemical equilibrium of small crystals. II. Solid particles embedded in a solid matrix. *Acta Metallurgica*, vol.30, pp.51-56.

Cammarata, R.C. (1994): Surface and interface stress effects in thin films. *Progress in Surface Science*, vol.46, pp.1-38.

Chen, K.H.; Kao, J.H.; Chen J.T. (2009): Regularized meshless method for antiplane piezoelectricity problems with multiple inclusions. *CMC: Computers, Ma-*

terials & Continua, vol. 9, pp. 253-280.

Cheng, H.C.; Hsu, Y.C.; Chen, W.H. (2009): The influence of structural defect on mechanical properties and fracture behaviors of carbon nanotubes. *CMC: Computers, Materials & Continua*, vol. 11, pp. 127-146.

Duan, H.L.; Wang, J.; Huang, Z.P.; Karihaloo, B.L. (2005): Size-dependent effective elastic constants of solids containing nanoinhomogeneities with interface stress. *Journal of the Mechanics and Physics of Solids*, vol.53, pp.1574-1596.

Gibbs, J.W. (1906): The Scientific Papers of J. Willard Gibbs. vol 1. Longmans-Green, London.

Gurtin, M.E.; Murdoch, A.I. (1975): A continuum theory of elastic material surfaces. *Archive for Rational Mechanics and Analysis*, vol. 57, pp.291-323.

Gurtin, M.E.; Weissmuller, J.; Larche, F. (1998): A general theory of curved deformable interfaces in solids at equilibrium. *Philosophical Magazine*, vol. 78, pp.1093-1109.

He, L.H.; Li, Z.R. (2006): Impact of surface stress on stress concentration. *International Journal of Solids and Structures*, vol. 43, pp.6208-6219.

Liang, X.H.; Wang, B.; Liu Y.L. (2009): Thickness effect of a thin film on the stress field due to the eigenstrain of an ellipsoidal inclusion. *International Journal of Solids and Structures*, vol. 46, pp. 322-330.

Lim, C.W.; Li, Z.R.; He, L.H. (2006): Size dependent, non-uniform elastic field inside a nano-scale spherical inclusion due to interface stress. *International Journal of Solids and Structures*, vol. 43, pp.5055-5065.

Miller, R.E.; Shenoy, V.B. (2000): Size-dependent elastic properties of nanosized structural elements. *Nanotechnology*, vol.11, pp.139-147.

Murdoch, A.I. (1976): Thermodynamical theory of elastic-material interfaces. *Quarterly Journal of Mechanics and Applied Mathematics*, vol. 29, pp.245-275.

Nix, W.D.; Gao, H. (1998): An atomistic interpretation of interface stress. *Scripta Materialia*, vol.39, pp.1653-1661.

Pao, Y.H.; Mow, C.C. (1973): Diffraction of elastic waves and dynamic stress concentration, Crane-Russak, New York.

Sharma, P.; Ganti, S.; Bhate, N. (2003): Effect of surfaces on the size-dependent elastic state of nano-inhomogeneities. *Applied Physics Letters*, vol. 82, pp.535-537.

Sharma, P.; Wheeler, L.T. (2007): Size-dependent elastic state of ellipsoidal nano-inclusions incorporating surface/interface tension. *ASME Journal of Applied Mechanics*, vol. 74, pp.447-454 .

Tian, L.; Rajapakse, R.K.N.D. (2007): Elastic field of an isotropic matrix with a nanoscale elliptical inhomogeneity. *International Journal of Solids and Structures*, vol.44, pp.7988-8005.

Wang, G.F.; Feng, X.Q.; Yu, S.W. (2007): Interface effects on the diffraction of plane compressional waves by a nanosized spherical inclusion. *Journal of Applied Physics*, vol.102, 043533.

Wang, G.F.; Wang, T.J.; Feng, X.Q. (2006): Surface effects on the diffraction of plane compressional waves by a nanosized circula hole. *Journal of Applied Physics*, vol. 89, 231923.

Wu, H.A.; Liu, G.R.; Wang, J.S. (2004): Atomistic and continuum simulation on extension behaviour of single crystal with nano-holes. *Modelling and Simulation in Materials Science and Engineering*, vol.12, pp.225-233.

Xie G.Q.; Long S.Y. (2006): Elastic vibration behaviors of carbon nanotubes based on micropolar mechanics. *CMC: Computers, Materials & Continua*, vol. 4, pp. 11-20.